Zielonka, J. , Zhao, H. , Xu, Y. & Kalyanaraman, B. Mechanistic similarities between oxidation of hydroethidine by Fremy's salt and superoxide: stopped-flow optical and EPR studies...

ARTICLE *in* FREE RADICAL BIOLOGY AND MEDICINE · NOVEMBER 2005

Impact Factor: 5.74 · DOI: 10.1016/j.freeradbiomed.2005.05.001 · Source: PubMed

Available online at www.sciencedirect.com

SCIENCE DIRECT

Free Radical Biology & Medicine 39 (2005) 853 – 863

www.elsevier.com/locate/freeradbiomed

Original Contribution

Mechanistic similarities between oxidation of hydroethidine by Fremy's salt and superoxide: Stopped-flow optical and EPR studies

Jacek Zielonka, Hongtao Zhao, Yingkai Xu, B. Kalyanaraman*

Department of Biophysics and Free Radical Research Center, Medical College of Wisconsin, 8701 Watertown Plank Road, P.O. Box 26509, Milwaukee, WI 53226, USA

Received 18 February 2005; revised 29 April 2005; accepted 3 May 2005

Abstract

We have previously shown that superoxide radical anion ($O_2^{\bullet-}$) reacts with hydroethidine (HE) to form a product that is distinctly different from ethidium (E^+) (Zhao et al., *Free Radic. Biol. Med.* **34:**1359; 2003). The structure of this product was recently determined as the 2-hydroxyethidium cation (2-OH-E^+) (Zhao et al., *Proc. Natl. Acad. Sci. USA* **102:**5727; 2005). In this study, using HPLC and mass spectrometry techniques, we show that 2-OH-E^+ is formed from the reaction between HE and nitrosodisulfonate radical dianion (NDS) or Fremy's salt. The reaction kinetics and mechanism were determined using steady-state and time-resolved optical and EPR techniques. Within the first 50 ms, an intermediate was detected. Another intermediate absorbing strongly at 460 nm and weakly at 670 nm was detected within a second. The structure of this species was assigned to an imino quinone derivative of HE. The stoichiometry of the reaction indicates that two molecules of NDS were needed to oxidize a molecule of HE. We postulate that the first step of the reaction involves the hydrogen atom abstraction from HE to form an aminyl radical that reacts with another molecule of NDS to form an adduct that decomposes to an imino quinone derivative of HE. A similar mechanism has been proposed for the reaction between HE and $O_2^{\bullet-}$. The reaction between HE and the Fremy's salt should provide a facile route for the synthesis of 2-OH-E^+, a diagnostic marker product of the HE/$O_2^{\bullet-}$ reaction.

Keywords: Hydroethidine; Fremy's salt; Nitrosodisulfonate radical dianion; Superoxide radical anion; 2-Hydroxyethidium; Fluorescent probes; Stopped flow; HPLC

Introduction

It is now generally believed that reactive oxygen species (ROS) are not only deleterious by-products of selected enzymatic and nonenzymatic processes, but are also important cell signaling intermediates [1,2]. Superoxide radical anion ($O_2^{\bullet-}$), the primary one-electron reduction product of molecular oxygen, triggers the formation of other ROS, such as H_2O_2, hydroxyl radical ($^{\bullet}OH$), and peroxyl radicals ($ROO^{\bullet}$). Thus, it is often difficult to attribute a particular signal transduction mechanism to a specific ROS [3]. This situation is further complicated by the fact that most extracellular ROS scavengers are not cell permeable. One of the factors that hampers our understanding of ROS in cell signaling and signal transduction mechanisms is the lack of specific cell-permeable diagnostic probes for $O_2^{\bullet-}$. It is essential that these probes are sensitive enough to detect low levels of ROS in cells without affecting the cellular function [4,5]. In this regard, the fluorescence technique is promising due to the availability of cell-permeable non-fluorescent probes that are trapped inside the cells by esterase-dependent hydrolysis, leading to the formation of characteristic fluorescent products during intracellular oxidative stress.

Recently, 5-ethyl-5,6-dihydro-6-phenyl-3,8-diaminophenanthridine (hydroethidine, HE, also known as dihydro-

Abbreviations: HE, hydroethidine; NDS, nitrosodisulfonate radical dianion; Fs, Fremy's salt; XO, xanthine oxidase; DTPA, diethylenetriamine pentaacetic acid; E^+, ethidium cation; 2-OH-E^+, 2-hydroxyethidium cation; ROS, reactive oxygen species; DMSO, dimethyl sulfoxide; TFA, trifluoroacetic acid.

* Corresponding author. Fax: +1 414 456 6512.
E-mail address: balarama@mcw.edu (B. Kalyanaraman).

0891-5849/$ - see front matter © 2005 Elsevier Inc. All rights reserved.
doi:10.1016/j.freeradbiomed.2005.05.001

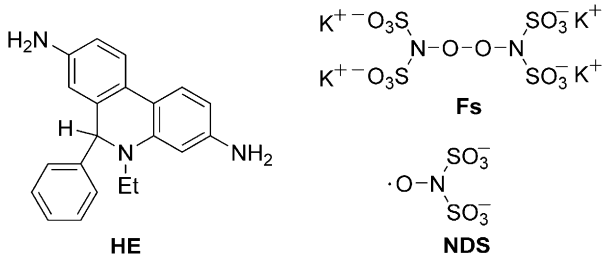

Fig. 1. Chemical structures. Chemical structures of hydroethidine (HE), Fremy's salt (Fs), and nitrosodisulfonate radical dianion (NDS).

ethidium, DHE) (Fig. 1) has been frequently used to detect the intracellular superoxide anion [6–8]. HE is formed from the reduction of ethidium cation (E^+), a well-known DNA intercalator [9,10]. HE is a neutral, cell-permeable molecule that accumulates in the cells [11,12]. As the reaction between HE and $O_2^{\bullet-}$ yields a characteristic "red fluorescence" [13–15], HE has been used to selectively image $O_2^{\bullet-}$ production in cells and tissues [6–8,16–19]. The major product of the HE/$O_2^{\bullet-}$ reaction was proposed to be the ethidium cation [20–22]. In some respects, the oxidative chemistry of HE is similar to dihydropyridines [23,24].

We have recently shown that the reaction of HE with $O_2^{\bullet-}$ yields a product that is structurally different from E^+ [25] and its structure was determined as the 2-hydroxyethidium cation (2-OH-E^+, Reaction 1) [26]. Surprisingly, this particular product is not formed from the reaction of HE with other biologically relevant oxidizing species (hydroxyl radical, peroxyl radicals, peroxynitrite, H_2O_2, and peroxidase), although these oxidants do react with HE to form other fluorescent products [27]. Based on the current knowledge, it appears that 2-OH-E^+ is a diagnostic marker product of $O_2^{\bullet-}$ reaction with HE. Thus, intracellular generation of $O_2^{\bullet-}$ can be detected and quantitated by monitoring formation of 2-OH-E^+ in cells incorporated with HE [5]. Another advantage of using HE as the intracellular superoxide probe is that unlike other probes used for $O_2^{\bullet-}$ detection, such as lucigenin, it does not artifactually stimulate $O_2^{\bullet-}$ production, although HE was reported to catalyze the dismutation of $O_2^{\bullet-}$ generated enzymatically [28]. Should this reaction occur in vivo, the HE assay may lead to an underestimation of the actual intracellular superoxide levels.

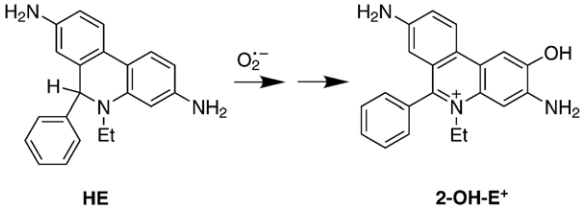

The objective of this study was to provide an independent synthetic route for 2-OH-E^+ that will facilitate the use of HE for quantitative detection of superoxide in biological systems. Furthermore, very little is known regarding the mechanism of reaction between superoxide and aromatic amino compounds. We used the Fremy's salt or potassium nitrosodisulfonate radical dianion (NDS, Fig. 1) to examine the mechanism of oxidation and hydroxylation of HE, as NDS has previously been used as a reagent for selective hydroxylation and oxidation of aromatic amines and phenols [29–31].

NDS is a product of dissociation of Fremy's salt (Fs, Fig. 1), a commercially available dimer of NDS. Fremy's salt is a source of a relatively stable, water-soluble nitroxyl radical that is widely used as an ESR standard for *g*-value determination and radical quantitation [29]. It has also been used as a model for peroxyl radicals in studies designed to investigate the antioxidant mechanism of action related to a wide range of natural products [32,33].

In this study, we demonstrate that Fremy's salt oxidizes HE to the same product, namely 2-OH-E^+, as does $O_2^{\bullet-}$. The similarities between the two reaction mechanisms are discussed. A facile route for an independent synthesis of 2-OH-E^+ is presented.

Materials and methods

Chemicals

Hydroethidine was purchased from Molecular Probes Inc. (Eugene, OR.). Xanthine oxidase from cow milk was from Roche Diagnostic GmbH (Mannheim, Germany). KH_2PO_4 and K_2HPO_4 were from Fisher Scientific (Fair Lawn, NJ). Ethidium bromide, potassium nitrosodisulfonate, xanthine, KD_2PO_4, K_2DPO_4, D_2O, DCl (35 wt %), $H_2{}^{18}O$, and other reagents were from Sigma-Aldrich (St. Louis, MO).

Hydroethidine stock solutions (15 mM) were prepared by dissolving known amounts of HE in deoxygenated DMSO under anaerobic conditions. The solution was then divided into several smaller aliquots and stored under argon at −20°C. Fresh HE solutions were prepared by dissolving the HE aliquots in 1 mM aqueous solution of HCl to minimize autoxidation. HE is more soluble and stable in acidic solutions than in neutral solutions. Solutions containing HE were protected from light before and during the experiments. The final concentration of HE was determined using the extinction coefficients, 1.8×10^4 and 9.75×10^3 M^{-1} cm^{-1} at 265 and 345 nm, respectively. These values were obtained from analyzing the optical spectra of the reduction product of ethidium bromide using $NaBH_4$ at several concentrations of E^+Br^- (0 – 100 μM).

Due to the instability of NDS in acidic solutions [34], stock solutions of NDS were generally prepared by dissolving Fremy's salt in phosphate buffer (100 mM, pH 7.5) containing 0.2 mM DTPA. The concentration of NDS

was determined using the extinction coefficients 1690 M^{-1} cm^{-1} (248 nm) and 20.8 M^{-1} cm^{-1} (545 nm) [34]. Typically, solutions of both reactants were mixed using equal volumes and the final concentrations of phosphate buffer (pH 7.4) and DTPA were 50 and 0.1 mM, respectively.

Fluorescence measurements

Fluorescence measurements were performed on a Shimadzu RF-5301PC spectrofluorophotometer (Shimadzu Scientific Instruments Inc., Japan). The excitation light wavelength was set at 356 nm for monitoring HE and at 470 nm for HE oxidation products. The slit widths were typically 3 and 5 nm for excitation and emission light, respectively.

UV-Vis absorption measurements

The UV-Vis absorption spectra were collected using an Agilent 8453 photodiode array spectrophotometer equipped with a thermostatted cell holder.

Determination of the extinction coefficient of 2-hydroxyethidium

To estimate the yield of the product of the reaction of Fremy's salt with HE, the effective extinction coefficient of 2-OH-E^+ at pH 7.4 was determined as follows: The reaction mixture containing xanthine (1.0 mM), xanthine oxidase (0.05 U/ml), and HE (the concentration range: 10 – 60 μM) in 50 mM phosphate buffer and 0.1 mM DTPA was incubated in the dark for 2 h with continuous O_2 bubbling. Following the incubation period, the UV-Vis absorption spectra of the reaction mixtures were collected and the amount of unreacted HE was determined by HPLC. The extinction coefficient 9.4×10^3 M^{-1} cm^{-1} at 470 nm was estimated assuming the amount of 2-OH-E^+ formed as being equal to the amount of reacted HE. We observed that 2-OH-E^+ undergoes deprotonation from the hydroxyl group at neutral pH, and therefore the estimated value should be regarded as an "effective" extinction coefficient at pH 7.4.

ESR measurements

ESR spectra were recorded at room temperature using a Bruker EMX spectrometer operating at 9.85 GHz and equipped with a Bruker ER 4119HS-WI high-sensitivity resonator. Typical spectrometer parameters were scan range, 100 G; time constant, 5.12 ms; sweep time, 5.12 s; modulation amplitude, 1.0 G; modulation frequency, 100 kHz; microwave power, 5.0 mW. Micropipettes (100 μl) were used as sample tubes. The intensity of the signal was calculated by summing the double integrals of three NDS ESR peaks.

Continuous flow and stopped-flow ESR measurements were carried out using the ESR equipment as above, but Bruker dielectric mixing resonator ER 4117 D-MVT was used. The solutions of both reactants in two syringes (gas-tight Hamilton, 10 ml) were driven simultaneously by a syringe pump via PEEK tubes (0.7 mm i.d.), through the mixer and sample tube inside the ESR cavity. The speed of the motor of the syringe pump was adjusted in 10 steps to obtain the mixture in the cavity of the age ranging from 15 ms to 1.5 s.

Stopped-flow measurements

Stopped-flow kinetic experiments were performed on Applied Photophysics 18MX stopped-flow spectrophotometer equipped with photodiode array (PDA) and photomultiplier (PM) for absorption and photomultiplier for fluorescence measurements. For characterizing spectral intermediates, the PDA detector was used, whereas PM detectors were used for kinetic analysis. To minimize photooxidation of HE by analyzing light during kinetic experiments, monochromator slits widths were set to 0.2 mm. For determining kinetic analysis of the fluorescence changes, cutoff filters were used to select the range of wavelengths of emission light (HE, λ_{exc} = 356 nm; cutoff filter, 400 nm; 2-OH-E^+: λ_{exc} = 470 nm; cutoff filter, 550 nm). To obtain the time-resolved fluorescence spectra, the emission light was passed through the second monochromator before reaching the PM.

Deuterium kinetic isotope effect

The hydrogen/deuterium kinetic isotope effect was determined by the reaction of HE (50 μM) with NDS (5 mM) in H_2O and D_2O. Solutions were prepared in a glove bag under an argon atmosphere. The HE solution was prepared and incubated for 1 h at room temperature using a 1 mM DCl in D_2O in order to achieve the hydrogen/deuterium exchange of the aromatic amino groups. Fremy's salt was dissolved in a $K_2DPO_4/KD_2PO_4/D_2O$ buffer. Analogous measurements were carried out in H_2O buffer, taking into account the relationship between the pH and the pD. The kinetics of the reaction was measured at 25°C using the stopped-flow technique. The value of the kinetic isotope effect was determined from three independent measurements.

Incorporation of the ^{18}O atom

To determine whether the oxygen atom in the HE/Fremy's salt reaction product originated from the solvent water, the reaction was performed in $H_2{}^{18}O$ by mixing 40 μl of $H_2{}^{18}O$ with 5 μl of 0.5 mM HE in 10 mM HCl/H_2O and 5 μl of phosphate buffer (100 mM, pH 7.5) containing NDS (1.0 mM) and 0.2 mM DTPA. The final concentration of $H_2{}^{18}O$ was therefore 80% (by volume). Control measure-

ments were carried out using $H_2{}^{16}O$ instead of $H_2{}^{18}O$. Incorporation of the oxygen atom into the product was checked using the HPLC/MS technique.

HPLC analysis

HE, E^+, HE, and Fremy's salt oxidation products were separated on an HPLC system Agilent 1100 equipped with fluorescence and UV-Vis absorption detectors. Typically, 50 μl of sample was injected into the HPLC system with a C_{18} column (Alltech, Kromasil, 250 × 4.6 mm, 5 μm) equilibrated with 10% CH_3CN (containing 0.1% (v/v) trifluoroacetic acid (TFA)) in 0.1% TFA aqueous solution. HE, E^+, and HE/$O_2^{\bullet-}$ product were separated by a linear increase in CH_3CN phase concentration from 10 to 70% in 46 min at a flow rate of 0.5 ml/min. Fluorescence detection at 260, 356, and 510 nm (excitation) and 595 nm (emission), as well as the absorptions at 210, 350, 370, 420, and 500 nm, were used to monitor the reaction products.

HPLC-mass spectrometry assay

Samples were analyzed by LC-ESI-MS (Agilent 1100 LC/MSD, SL model). Samples (2 μl) were separated on a reversed-phase C_{18} column (Phenomenex, Jupiter, 250 × 2 mm, 5 μm, 100 Å) using water with 0.1% formic acid and CH_3CN with 0.1% (v/v) formic acid as a mobile phase at a flow rate of 0.2 ml/min. The mobile phase started at 10% CH_3CN and linearly increased to 100% CH_3CN over 80 min. The drying gas flow was 12 L/min, drying gas temperature was 300°C, nebulizer pressure was 35 psig, vaporizer temperature was 325°C, capillary voltage was 3000 V, and fragmentor voltage was 90 V. Detection was made in the positive mode for the *m/z* range of 200–850.

Synthesis of 2-hydroxyethidium (2-OH-E^+)

The synthesis of 2-OH-E^+ was performed in two steps. First, E^+ was reduced to HE, which was then oxidized to 2-OH-E^+. In step 1, 100 mg (0.25 mmol) of E^+Br^- was reduced to HE using $NaBH_4$ according to a known procedure [9]. The product was purified using a silica gel column in the dark. During the next step, a solution of Fremy's salt (19.6 mg, 0.073 mmol) dissolved in a phosphate buffer (50 ml, pH 7.4, 0.1 M) was slowly added to a solution of hydroethidine (10 mg, 0.032 mmol) in 500 ml of phosphate buffer (0.1 M, pH 7.4) while stirring in the dark. The reaction mixture was continuously stirred for 30 min. The reaction mixture was then filtered and extracted with a mixture of chloroform and methanol (ratio 2:1, 100 ml × 5). The product was purified using a silica gel column (prewashed with chloroform) with methanol as an eluent and the second band was collected. After removing the solvent in vacuo, a red-orange colored product was obtained.

Unless otherwise stated, the accuracy of the determination of rate constants and extinction coefficients lies within a limit of ±10%.

Results

Identification of the product of NDS reaction with hydroethidine

Nitrosodisulfonate radical dianion reacts with hydroethidine to give a product eluting at a retention time the same as the product of the reaction of HE with superoxide radical anion (Fig. 2). The structure of this product was confirmed using the HPLC/MS (Fig. 3) technique. Thus, NDS reacts with hydroethidine to form the 2-hydroxyethidium cation, a diagnostic marker product of the reaction between HE and $O_2^{\bullet-}$.

Kinetics of the reaction

The reaction kinetics was followed by observing the changes in concentrations of both reactants and products using UV-Vis absorption, fluorescence, and EPR techniques (Figs. 4A–D). The changes in the concentration of NDS were measured by EPR (Fig. 4B), whereas HE decay and 2-OH-E^+ formation were detected by fluorescence (excitation wavelength 356 nm for HE, Fig. 4C; excitation wavelength 470 nm for 2-OH-E^+, Fig. 4D).

Using an excess of NDS, the pseudo-first-order conditions have been obtained and the rate constant has been

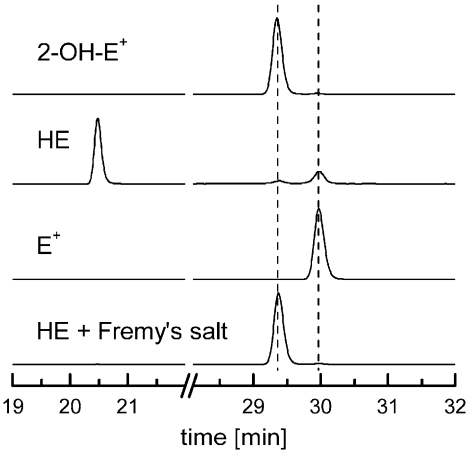

Fig. 2. HPLC analysis of the HE/Fremy's salt reaction. HE (16 μM) was added to solution containing NDS (32 μM) in phosphate buffer (pH 7.4, 50 mM) and incubated for 60 min. HPLC traces were obtained from solutions containing E^+ (16 μM), HE (16 μM), and 2-OH-ethidium formed from an incubation mixture containing HE (16 μM), xanthine (1.0 mM), and xanthine oxidase (0.05 U/ml) in phosphate buffer. Incubation mixtures were analyzed by HPLC with a fluorescence detector using an excitation wavelength 510 nm and emission wavelength 595 nm, as described under Materials and methods. Because of the differences in the fluorescence intensities of the products analyzed, the scale was set differently for each HPLC trace.

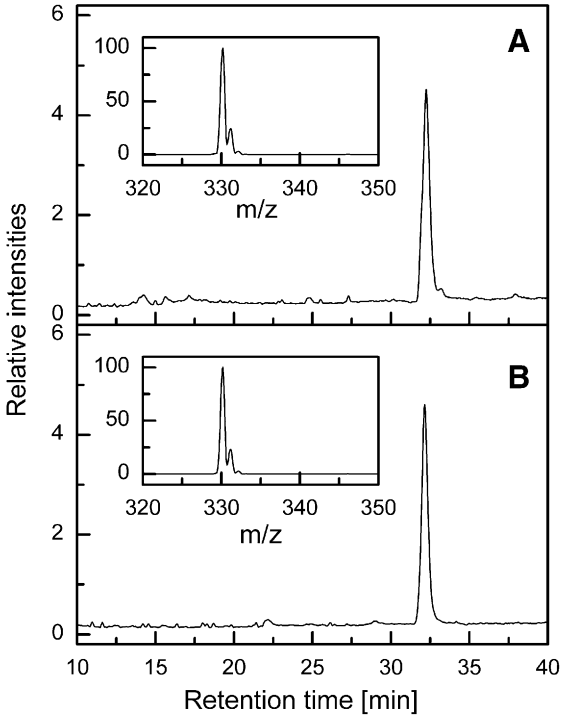

Fig. 3. HPLC/mass spectrum of the product of the HE/Fremy's salt reaction. (A) HPLC/MS trace (total ionic current, TIC) of the reaction mixture of HE (50 μM) with NDS (100 μM) in aqueous solution containing phosphate buffer (pH 7.4, 50 mM) and DTPA (100 μM) incubated for 50 min. Inset: MS spectrum of the product isolated from the reaction mixture by the procedure described under Materials and methods. (B) HPLC/MS trace (TIC) of the reaction mixture of HE (50 μM) with xanthine (1.0 mM) and XO (50 mU/ml) in aqueous solution containing phosphate buffer (pH 7.4, 50 mM) and DTPA (100 μM) incubated for 80 min and bubbled continuously with O_2. Inset: MS spectrum of the product eluting at 32.2 min retention time.

evaluated using a stopped-flow technique. Using this technique the decay of HE was observed by monitoring the disappearance of the fluorescence band at 420 nm (excitation light: 356 nm). The dependence of the observed pseudo-first-order rate constant on the NDS concentration was linear and gave the second-order rate constant of 5.8×10^2 M^{-1} s^{-1}. This value has been also confirmed using the stopped-flow EPR measurements, where the kinetics of NDS decay was observed using a twofold excess of NDS.

Stoichiometry of the reaction

To establish the mechanism of the reaction, its stoichiometry has been investigated using EPR spectroscopy to monitor changes in NDS concentration (Figs. 5A and 5B). A HPLC technique was used to monitor the concentration of HE and 2-OH-E^+ (Fig. 5C). As shown in Fig. 5A, the intensity of the EPR signal of NDS (Fig. 5A, top) decreased in the presence of HE (Fig. 5A, bottom). Fig. 5B shows the changes in the EPR intensity of NDS as a function of NDS concentration in the absence and presence of HE. The amount of Fremy's salt concentration was monitored at a reaction time equal to 5 half-lifetimes ($t_{1/2}$) using the previously determined rate constant. At longer incubation times, we observed an additional consumption of NDS, indicating that the reaction product is also capable of reacting with NDS. Similar results were obtained using the HPLC technique (Fig. 5C). The data shown indicate that NDS must be present at two times higher concentration than HE to consume all of it. Also, the yield of 2-OH-E^+ initially increased with increasing NDS concentration up to twofold excess; at higher NDS concentrations the 2-OH-E^+ yield started to decrease (Fig. 5C).

The absolute yield of 2-OH-E^+ formed during the reaction was estimated on the basis of the determined extinction coefficient of the product at 470 nm at pH 7.4. On the basis of the stoichiometry of the reaction, the yield of 2-OH-E^+ in the reaction of HE with NDS was estimated to be nearly 100%, indicating a quantitative conversion of HE to 2-OH-E^+.

Detection of reaction intermediates

The reaction intermediates were detected using the stopped-flow technique. As shown in Figs. 6 and 7, within the first second after mixing NDS and HE, there was an increase in the intensity of the absorption bands at 460 nm, 670 nm, and below 330 nm. Simultaneously, a decrease in the intensity of the absorption band at 350 nm was observed. After 2.5 s, the absorption band intensity at 670 nm decreased, the intensity of the band at 460 nm slightly decreased,and the maximum wavelength was red-shifted by 10 nm. An additional increase in the absorbance below 330 nm was also observed. We attribute the decrease in the absorption at 350 nm to the decay of HE and the transient intermediate formed from HE. The increase in the absorption at 460 and 670 nm we assign to an imino quinone species derived from HE.

Comparison between the HE fluorescence decay and the change in the absorption at 350 nm (Fig. 8) clearly indicates that an intermediate was formed that absorbs light at the same wavelength. The initial increase in absorbance at 350 nm can only be observed at NDS concentrations in the millimolar range; at lower NDS concentrations, the steady-state levels of the intermediate are probably too low because of a much slower rate of formation as compared to its decay rate. During further decay of HE there was a decrease in absorbance at 350 nm accompanied by an increase in the absorbance at 460 and 670 nm. This second intermediate reaches a maximum concentration at 0.8 s after mixing of the reactants under these conditions. After 2 s, the transient product disappeared and another product absorbing at 470 nm was formed. Formation of this product was also observed by its fluorescence using the excitation at 470 nm and by UV absorption changes. The product formed was more persistent at lower NDS concentrations (<twofold). At higher NDS concentrations, this fluorescent product also started to decrease. The time-resolved fluorescence spectra

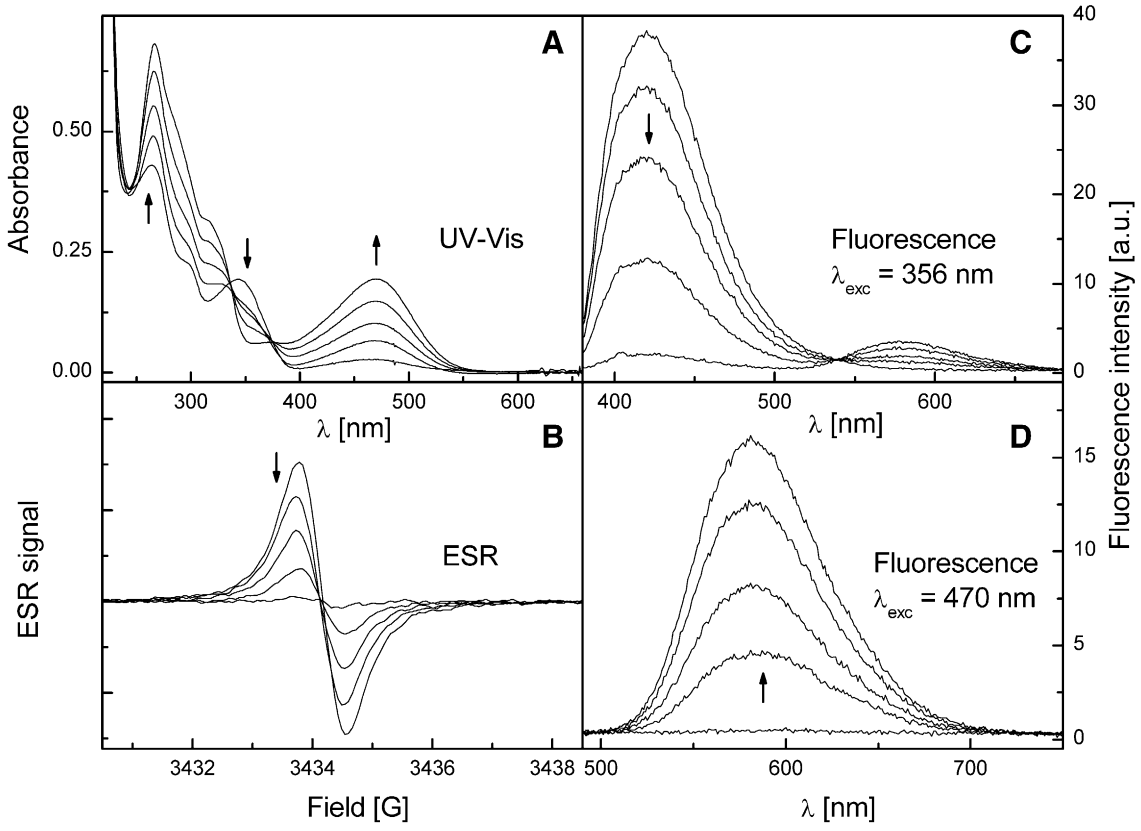

Fig. 4. Spectral changes accompanying the reaction of Fremy's salt with HE. *(*A) UV-Vis absorption spectra during the reaction of HE (20 μM) with NDS (40 μM). (B) The decay of the ESR absorption due to NDS during the reaction of 20 μM NDS with 40 μM HE. For picture clarity only the central line of NDS ESR spectrum is shown. (C) Fluorescence spectral changes using excitation wavelength 356 nm during the reaction of HE (20 μM) with NDS (40 μM). (D) Fluorescence spectral changes using excitation wavelength 470 nm during the reaction of HE (20 μM) with NDS (40 μM). The presented spectra were collected during the first 6 min of the reaction. Arrows indicate the direction of the spectral changes during the reaction.

show the formation of a fluorescence band with a maximum in the wavelength range, i.e., 570 – 590 nm (in the presence of the excitation light at 470 nm), while the fluorescence band at 420 nm (excitation at 356 nm) decayed. This fluorescent product was assigned to 2-OH-E^+. The dependence of its stability on NDS concentration is in agreement with the established reaction stoichiometry, indicating that the product could be further oxidized in the presence of excess NDS.

In order to detect the paramagnetic intermediate(s), the continuous flow ESR cavity was used, which allowed the spectral scanning of several reagent mixtures at various time intervals. However, no paramagnetic species other than NDS could be detected under different reaction conditions (data not shown). In addition, attempts to spin trap the radical intermediate using BMPO (5 mM) and POBN (50 mM) were unsuccessful. These results suggest that if the radical species were formed during the reaction, their rates of decay must have been much faster than the rates of formation, thus keeping their steady-state concentrations below the EPR detection limit.

To investigate whether E^+ was formed as an intermediate during the conversion of HE to 2-OH-E^+, the reaction between E^+ and Fremy's salt was performed. Formation of 2-OH-E^+ was not observed, indicating that E^+ is not formed as an intermediate during the reaction of HE with NDS (data not shown).

Origin of the oxygen atom in 2-OH-E^+

During the reaction between NDS and HE, an oxygen atom is incorporated into the product, 2-OH-E^+. The oxygen atom can be derived from water, molecular oxygen, or Fremy's salt. We tested the following possibilities. HE (50 μM) was reacted with NDS (100 μM) in the deoxygenated solutions to investigate the possibility whether dissolved molecular oxygen plays a role. HPLC results indicate that 2-OH-E^+ yield was not significantly affected (data not shown). In addition, the reaction kinetics, as measured using the stopped-flow technique (50 μM HE, 5 mM NDS), were the same in the presence and absence of oxygen. To check whether the oxygen atom in 2-OH-E^+ is derived from water, the reaction was carried out in $H_2{}^{18}O$ (80% by volume). No incorporation of ^{18}O atom into the product could be detected by using the HPLC/MS technique. On the basis of these results, we conclude that the oxygen atom in 2-OH-E^+ originated from NDS during the oxidation of HE by NDS.

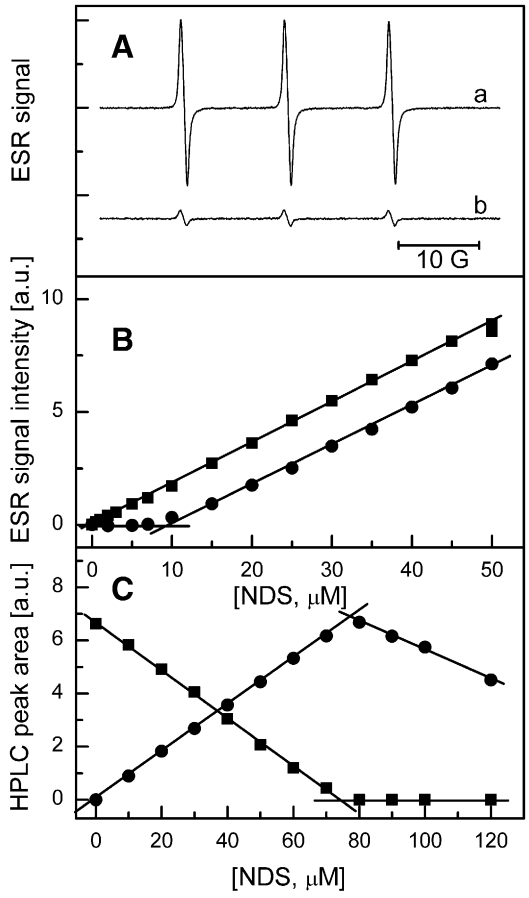

Fig. 5. Measurement of the stoichiometry of the reaction between HE and Fremy's salt. (A) ESR spectrum of NDS (20 μM) in the absence (a) and presence (b) of HE (10 μM). (B) ESR signal intensity (after double integration) of NDS as a function of its concentration in the absence (■) and presence (●) of HE. HE concentration: 5 μM. (C) HPLC peak area of (■) HE (λ_{exc} = 356 nm, λ_{obs} = 595 nm, peak at 19.6 min) and (●) 2-OH-E^+ (λ_{exc} = 510 nm, λ_{obs} = 595 nm, peak at 28.7 min) as a function of NDS concentration. The peak areas of 2-OH-E^+ have been scaled by a factor of 0.1 to fit on the same scale as HE peak area. HE concentration: 40 μM.

Deuterium kinetic isotope effect

To determine the site of occurrence of the initial hydrogen abstraction from HE by NDS, we performed the oxidation reaction in deuterium oxide. The deuterium kinetic isotope effect, defined as k_H/k_D, was determined to be 1.9 ± 0.1 at 25°C, as measured by the decay of HE fluorescence using the stopped-flow technique. The observed isotope effect is close to that observed for oxidation of aniline by ferrate (VI) in aqueous solution [35] and slightly lower than the effect observed during oxidation of diphenylamine by primary alkyl radicals at 100°C in *n*-dodecane solution [36]. It is likely that all the aromatic amino hydrogens are replaced by the deuterium. The observed isotope effect of 1.9 suggests that the N–H bond scission is more probable during the first step of the oxidation of HE by NDS. The determined value of k_H/k_D cannot be viewed as a primary deuterium isotope effect, as it is a product of the primary, the secondary, and the solvent effects. Indeed, it is plausible that the solvent effect contributes to the observed value, as there was an increase in the fluorescence intensity of HE in D_2O as compared to H_2O. This indicates that the difference in the strength of solvent–solute interactions observed in H_2O promotes the nonradiative decay of the excited state of HE. This effect had previously been reported for aniline [37].

Discussion

The present data indicate that the nitrosodisulfonate radical dianion, a stable nitroxyl radical, reacts with HE to form the 2-OH-E^+, a superoxide-specific marker product of HE. The identity of the product was confirmed by UV-Vis, fluorescence, HPLC, and MS techniques. The presence of the isosbestic points in the UV-Vis absorption, the fluorescence spectra, the single peak observed in HPLC data, and the product yield are all indicative of the fact that 2-hydroxyethidium is the only product of the reaction. This reaction provides a facile route for a nonenzymatic synthesis of 2-OH-E^+. As this product is selectively formed from the reaction between superoxide and HE, it is important to establish the mechanism of formation of this product in a related chemical system. In this study, we showed that the rate constant for the reaction between HE and NDS is $k = 5.8 \times 10^2$ M^{-1} s^{-1} and that the stoichiometry of this reaction is 2:1 (i.e., two molecules of NDS are consumed by a molecule of HE to form the 2-OH-E^+). Although this rate constant is considerably lower than that of the reaction between HE and $O_2^{\bullet-}$ ($k \sim 10^5$ M^{-1} s^{-1} [25]), the enhanced stability of NDS at pH 7.4 made it possible to investigate the kinetics of this reaction using the stopped-flow technique.

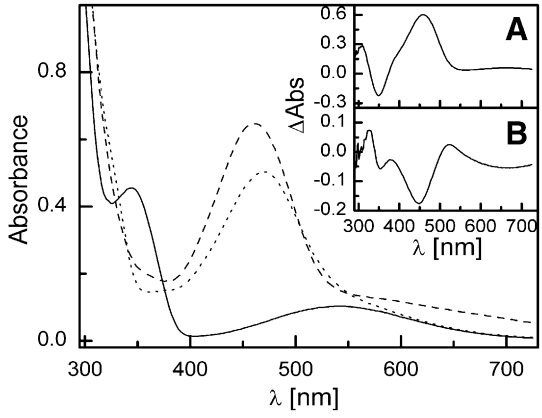

Fig. 6. Time-resolved absorption spectra measured during stopped-flow experiments. The spectra were collected 4 ms (solid line), 0.8 s (dashed line), and 3.0 s (dotted line) after mixing using PDA detector. Initial concentrations after mixing: 50 μM HE and 5.0 mM NDS, 50 mM phosphate buffer, 0.1 mM DTPA. T = 25°C, optical pathlength l = 1.0 cm. Insets: (A) Differential absorption spectrum obtained after subtraction of the spectrum collected after 4 ms from the spectrum collected after 0.8 s. (B) Differential absorption spectrum obtained after subtraction of the spectrum collected after 0.8 s from the spectrum collected after 3.0 s.

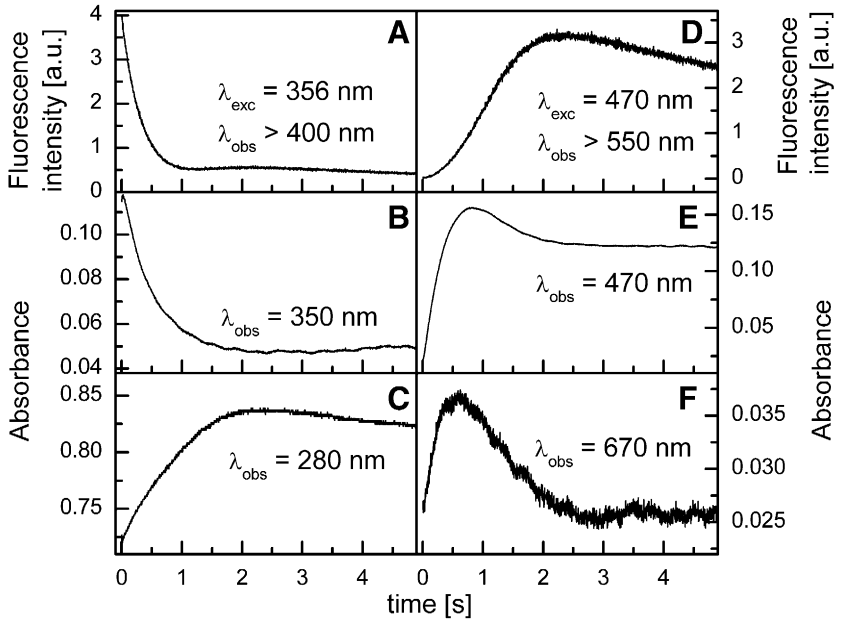

Fig. 7. Stopped-flow kinetics measurements of the HE/Fremy's salt reaction. Initial concentrations after mixing HE and NDS in 50 mM phosphate buffer containing 0.1 mM DTPA are 50 μM HE and 5.0 mM NDS. Measurements were made at $T = 25°C$ using an optical pathlength $l = 0.2$ cm. (A) HE fluorescence decay ($\lambda_{exc} = 356$ nm, $\lambda_{obs} > 400$-nm-cutoff filter); (B) absorbance changes at $\lambda_{obs} = 350$ nm; (C) absorbance changes at $\lambda_{obs} = 280$ nm; (D) 2-OH-E^+ fluorescence changes, ($\lambda_{exc} = 470$ nm, $\lambda_{obs} > 550$-nm-cutoff filter); (E) absorbance changes at $\lambda_{obs} = 470$ nm; (F) absorbance changes at $\lambda_{obs} = 670$ nm.

As indicated earlier, two molecules of NDS are consumed per one molecule of HE to form one molecule of the product, 2-OH-E^+. On the basis of the 2:1 stoichiometry, we propose that the radical formed in the first step of the reaction (Reaction 2) reacts with another NDS molecule (Reaction 3).

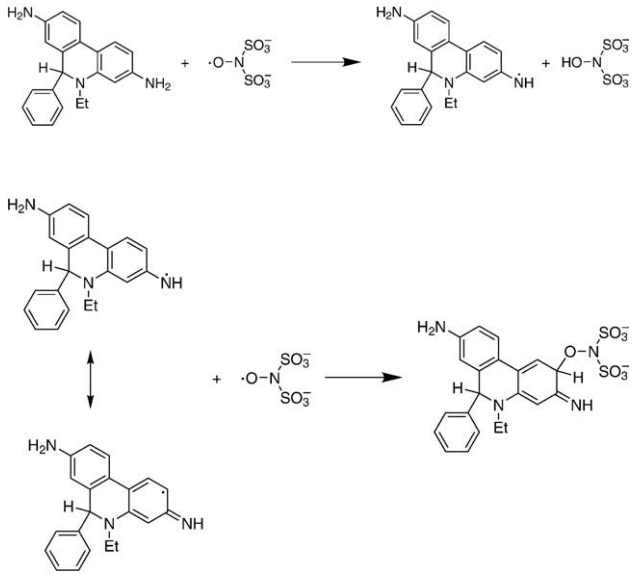

The first step of the reaction involves a hydrogen atom abstraction from the amine group to give an aromatic aminyl radical of HE. This reaction may proceed through a hydrogen atom or an electron-proton transfer. The observed

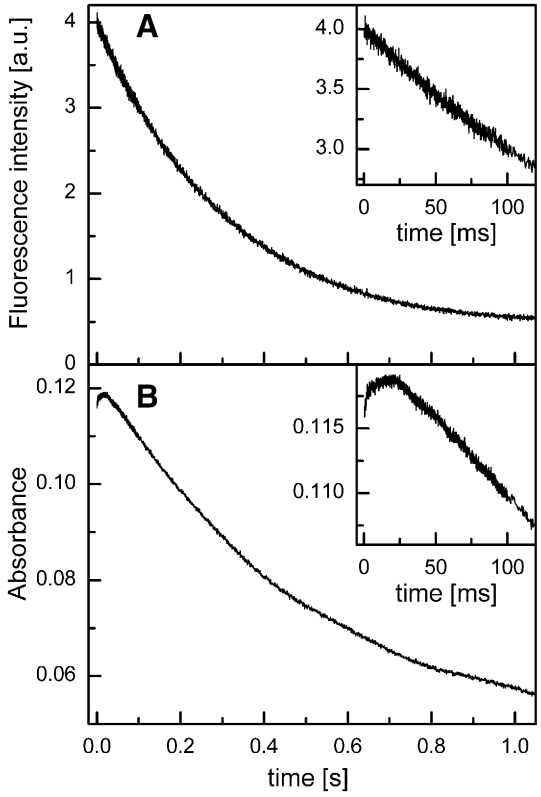

Fig. 8. Stopped-flow kinetics measurements within the first second. Kinetic traces were obtained within 1 safter mixing of HE with NDS. Initial concentrations after mixing: 50 μM HE and 5.0 mM NDS, 50 mM phosphate buffer, 0.1 mM DTPA. $T = 25°C$, optical pathlength = 0.2 cm. (A) HE fluorescence decay, ($\lambda_{exc} = 356$ nm, $\lambda_{obs} > 400$ nm – cut off filter); (B) absorbance changes at $\lambda_{obs} = 350$ nm, $l = 0.2$ cm. Inset: magnification of the traces obtained after the first 120 ms after mixing.

deuterium kinetic isotope effect, however, leads us to conclude that the first step involves the abstraction of a hydrogen atom from the exchangeable aromatic amino protons. Although we could not detect the initial radical by time-resolved ESR or spin trapping, this may be due to the significantly higher rate of its decay (via radical – radical recombination mechanism) as compared to its rate of formation. Indeed, even in the presence of a 4-fold excess of HE in the reaction mixture, when NDS would be consumed during the first step, there was no deviation from the linearity of the product yield as a function of NDS concentration (Fig. 5C). On the basis of the mechanisms previously postulated for the NDS reaction with aromatic amines [30], we propose that the reaction between the primary aminyl radical and the NDS gives an adduct that then decomposes in a subsequent reaction to give the quinone imine product (Reaction 4). The final product 2-OH-E^+ is formed from the quinone imine following a tautomerization/protonation mechanism (Reaction 5).

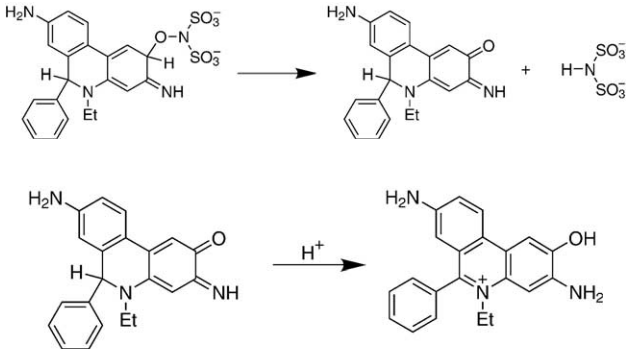

As the transition state for intramolecular tautomerization is likely to be energetically unfavorable due to geometric restrictions, it is plausible that the isomerization reaction occurs via a bimolecular mechanism involving a hydride acceptor (Reaction 5a) or a hydride donor (Reaction 5b). Although we propose that the hydride transfer occurs prior to protonation, the possibility that the quinone imine derivative of HE undergoes protonation prior to hydride transfer (Reaction 5b) cannot be excluded.

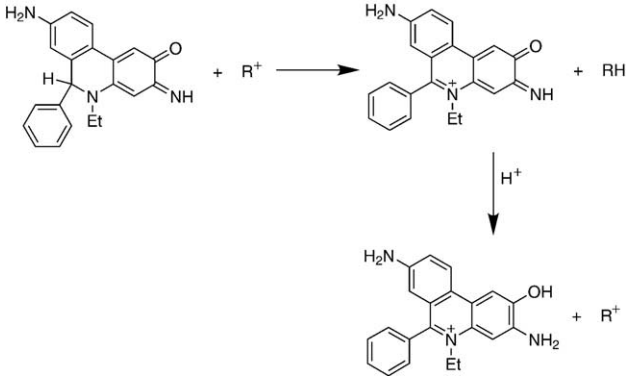

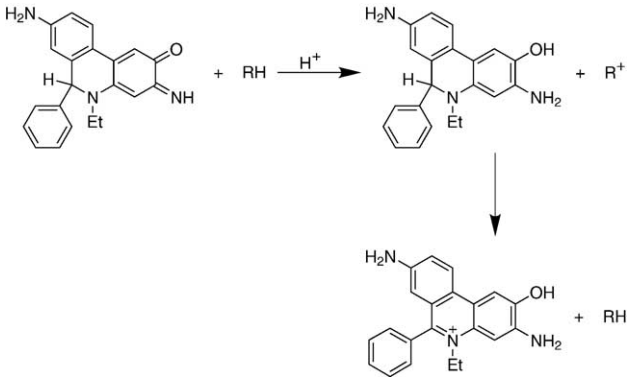

We also tentatively postulate the formation of a quinone imine product that absorbs at 460 and 670 nm within the first second of the reaction, whereas the rapid increase in the initial absorbance at 350 nm we attribute to the product of the reaction between the NDS and the HE-derived radical.

On the basis of the mechanisms proposed for the reaction of NDS with HE leading to 2-OH-E^+, we propose that the mechanism of the reaction of HE with superoxide radical may involve at first the HE aminyl radical formation (Reaction 6). Involvement of a radical intermediate during this reaction had previously been suggested [28].

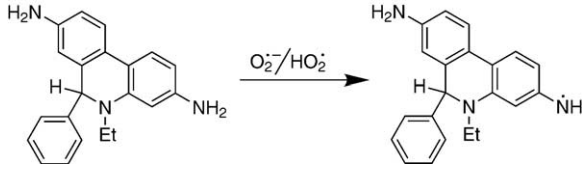

The present results, combined with the known mechanism for the reaction between superoxide and phenoxyl-type radicals [38], prompted us to postulate Reaction 7, i.e., the radical-radical recombination between the aminyl radical formed during the first step and the superoxide anion to form a hydroperoxide derivative. The subsequent reaction involves an elimination of a water molecule, forming the quinone imine (Reaction 8). The possible mechanisms of formation of 2-OH-E^+ from the quinone imine are shown in Reaction 5.

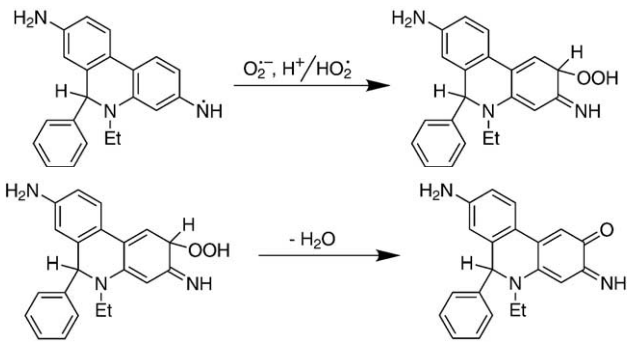

As other ROS also may react with HE to form an aminyl radical, the specific formation of 2-OH-E^+ in the case of $O_2^{\bullet -}$ is dependent on the secondary reaction between the superoxide and the aminyl radical to form the 2-quinone-3-imine derivative of HE. The formation of the aminyl radical in the first step of the reaction may explain why HE does not by itself induce $O_2^{\bullet -}$ formation. The aromatic aminyl radicals do not typically reduce oxygen to superoxide [39].

In conclusion, our study indicates that 2-hydroxyethidium, a specific marker product formed from the intracellular superoxide/HE reaction, also can be independently synthesized by the oxidation of HE using Fremy's salt. We propose that the conversion of HE to 2-OH-E^+ involves the intermediate formation of an aminyl radical and the quinone imine species.

Acknowledgments

This work was supported by NIH Grants 5RO1HL067244, 2RO1NS39958, and 5PO1HL68769-01.

References

[1] Thannickal, V. J.; Fanburg, B. L. Reactive oxygen species in cell signaling. *Am. J. Physiol.* **279:**L1005–L1028; 2000.

[2] Dröge, W. Free radicals in the physiological control of cell function. *Physiol. Rev.* **82:**47–95; 2002.

[3] Halliwell, B.; Gutteridge, J. M. C. *Free Radicals in Biology and Medicine, third ed.* Oxford: Oxford Univ. Press; 1999.

[4] Tarpey, M. M.; Wink, D. A.; Grisham, M. B. Methods for detection of reactive metabolites of oxygen and nitrogen: in vitro and in vivo considerations. *Am. J. Physiol. Regul. Integr. Comp. Physiol.* **286:**R431–R444; 2004.

[5] Fridovich, I. Editorial commentary on "Superoxide reacts with hydroethidine but forms a fluorescent product that is distinctly different from ethidium: potential implications in intracellular fluorescence detection of superoxide" by H. Zhao et al. *Free Radic. Biol. Med.* **34:**1357–1358; 2003.

[6] Hwang, J.; Saha, A.; Boo, Y. C.; Sorescu, G. P.; McNally, J. S.; Holland, S. M.; Dikalov, S.; Giddens, D. P.; Griendling, K. K.; Harrison, D. G.; Jo, H. Oscillatory shear stress stimulates endothelial production of O_2^- from $p47^{phox}$-dependent NAD(P)H oxidases, leading to monocyte adhesion. *J. Biol. Chem.* **278:**47291–47298; 2003.

[7] Han, D.; Antunes, F.; Canali, R.; Rettori, D.; Cadenas, E. Voltage-dependent anion channels control the release of the superoxide anion from mitochondria to cytosol. *J. Biol. Chem.* **278:**5557–5563; 2003.

[8] Budd, S. L.; Castilho, R. F.; Nicholls, D. G. Mitochondrial membrane potential and hydroethidine-monitored superoxide generation in cultured cerebellar granule cells. *FEBS Lett.* **415:**21–24; 1997.

[9] Thomas, G.; Roques, B. Proton magnetic resonance studies of ethidium bromide and its sodium borohydride reduced derivative. *FEBS Lett.* **26:**169–175; 1972

[10] Olmsted III, J.; Kearns, D. R. Mechanism of ethidium bromide fluorescence enhancement on binding to nucleic acids. *Biochemistry* **16:**3647–3654; 1977.

[11] Bucana, C.; Saiki, I.; Nayar, R. Uptake and accumulation of the vital dye hydroethidine in neoplastic cells. *J. Histochem. Cytochem.* **34:**1109–1115; 1986.

[12] Saiki, I.; Bucana, C. D.; Tsao, J. Y.; Fidler, I. J. Quantitative fluorescent microassay for identification of antiproliferative compounds. *J. Natl. Cancer Inst.* **77:**1235–1240; 1986.

[13] Rothe, G.; Valet, G. Flow cytometric analysis of respiratory burst activity in phagocytes with hydroethidine and 2′,7′-dichlorofluorescin. *J. Leukoc. Biol.* **47:**440–448; 1990.

[14] Carter, W. O.; Narayanan, P. K.; Robinson, J. P. Intracellular hydrogen peroxide and superoxide anion detection in endothelial cells. *J. Leukoc. Biol.* **55:**253–258; 1994.

[15] Bindokas, V. P.; Jordán, J.; Lee, C. C.; Miller, R. J. Superoxide production in rat hippocampal neurons: selective imaging with hydroethidine. *J. Neurosci.* **16:**1324–1336; 1996.

[16] Endl, E.; Steinbach, P.; Hofstädter, F. Flow cytometric analysis of cell suspensions exposed to shock waves in the presence of the radical sensitive dye hydroethidine. *Ultrasound Med. Biol.* **21:**569–577; 1995.

[17] Düssmann, H.; Kögel, D.; Rehm, M.; Prehn, J. H. M. Mitochondrial membrane permeabilization and superoxide production during apoptosis. *J. Biol. Chem.* **278:**12645–12649; 2003.

[18] Bindokas, V. P.; Kuznetsov, A.; Sreenan, S.; Polonsky, K. S.; Roe, M. W.; Philipson, L. H. Visualizing superoxide production in normal and diabetic rat islets of langerhans. *J. Biol. Chem.* **278:**9796–9801; 2003.

[19] Peterson, S. L.; Morrow, D.; Liu, S.; Liu, K. J. Hydroethidine detection of superoxide production during the lithium-pilocarpine model of status epilepticus. *Epilepsy Res.* **49:**226–238; 2002.

[20] Kobzik, L.; Godleski, J. J.; Brain, J. D. Oxidative metabolism in the alveolar macrophage: analysis by flow cytometry. *J. Leukoc. Biol.* **47:**295–303; 1990.

[21] Al-Mehdi, A. B.; Shuman, H.; Fisher, A. B. Intracellular generation of reactive oxygen species during nonhypoxic lung ischemia. *Am. J. Physiol.* **272:**L294–L300; 1997.

[22] Narayanan, P. K.; Goodwin, E. H.; Lehnert, B. E. α Particles initiate biological production of superoxide anions and hydrogen peroxide in human cells. *Cancer Res.* **57:**3963–3971; 1997.

[23] Zielonka, J.; Marcinek, A.; Adamus, J.; Gębicki, J. Direct observation of NADH radical cation generated in reactions with one-electron oxidants. *J. Phys. Chem. A* **107:**9860–9864; 2003.

[24] Gębicki, J.; Marcinek, A.; Zielonka, J. Transient species in the stepwise interconversion of NADH and NAD^+. *Acc. Chem. Res.* **37:**379–386; 2004.

[25] Zhao, H.; Kalivendi, S.; Zhang, H.; Joseph, J.; Nithipatikom, K.; Vasquez-Vivar, J.; Kalyanaraman, B. Superoxide reacts with hydroethidine but forms a fluorescent product that is distinctly different from ethidium: potential implications in intracellular fluorescence detection of superoxide. *Free Radic. Biol. Med.* **34:**1359–1368; 2003.

[26] Zhao, H.; Joseph, J.; Fales, H. M.; Sokoloski, E. A.; Levine, R. L.; Vasques-Vivar, J.; Kalyanaraman, B. Detection and characterization of the product of hydroethidine and intracellular superoxide by HPLC and limitations of fluorescence. *Proc. Natl. Acad. Sci. USA* **102:**5727–5732; 2005.

[27] Zhao, H. *Detection of superoxide by ESR-spin trapping and hydroethidine fluorescence.* Ph.D. dissertation submitted to the Medical College of Wisconsin; 2004.

[28] Benov, L.; Sztejnberg, L.; Fridovich, I. Critical evaluation of the use of hydroethidine as a measure of superoxide anion radical. *Free Radic. Biol. Med.* **25:**826–831; 1998.

[29] Weil, J. A.; Bolton, J. R.; Wertz, J. E. *Electron paramagnetic resonance: elementary theory and practical applications*. New York: Wiley-Interscience; 1994.

[30] Zimmer, H.; Lankin, D. C.; Horgan, S. W. Oxidations with potassium nitrosodisulfonate (Fremy's radical). The Teuber reaction. *Chem. Rev.* **71:**229–246; 1971.

[31] Palmisano, G.; Danielli, B.; Lesma, G.; Trupiano, F. Oxidation

of β-anilinoacrylate alkaloids vincadifformine and tabersonine by Fremy's salt. A Mechanistic insight into the rearrangement of *Aspidosperma* to *Hunteria* alkaloids. *J. Org. Chem.* **53:** 1056–1064; 1988.

[32] Liu, Z.-L.; Han, Z.-X.; Chen, P.; Liu, Y.-C. Stopped-flow ESR study on the reactivity of vitamin E, vitamin C and its lipophilic derivatives towards Fremy's salt in micellar systems. *Chem. Phys. Lipids* **56:**73–80; 1990.

[33] Holler, T. P.; Hopkins, P. B. Ovothiols as free-radical scavengers and the mechanism of ovothiol-promoted NAD(P)H-O_2 oxidoreductase activity. *Biochemistry* **29:**1953–1961; 1990.

[34] Murib, J. H.; Ritter, D. M. Decomposition of nitrosyl disulfonate ion. I. Products and mechanism of color fading in acid solution. *J. Am. Chem. Soc.* **74:**3394–3398; 1952.

[35] Huang, H.; Sommerfeld, D.; Donn, B. C.; Lloyd, C. R.; Eyring, E. M. Ferrate(VI) oxidation of aniline. *J. Chem. Soc., Dalton Trans.,*1301–1305; 2001.

[36] Burton, A.; Ingold, K. U.; Walton, J. C. Absolute rate constants for the reactions of primary alkyl radicals with aromatic amines. *J. Org. Chem.* **61:**3778–3782; 1996.

[37] Tobita, S.; Ida, K.; Shiobara, S. Water-induced fluorescence quenching of aniline and its derivatives in aqueous solution. *Res. Chem. Intermed.* **27:**205–218; 2001.

[38] Winterbourn, C. C.; Kettle, A. J. Radical-radical reactions of superoxide: a potential route to toxicity. *Biochem. Biophys. Res. Commun.* **305:**729–736; 2003.

[39] Alfassi, Z. B., ed. *The Chemistry of N-Centered Radicals*. New York: Wiley; 1998.